

From bi-layer to tri-layer Fe nanoislands on $\text{Cu}_3\text{Au}(001)$.

A. Verdini, L. Floreano,* F. Bruno, D. Cvetko,^a A. Morgante,^b

Laboratorio TASC dell'Istituto Nazionale per la Fisica della Materia, S.S.14 Km.163.5, Basovizza, I-34012 Trieste, Italy

^a *also at: J. Stefan Institute, University of Ljubljana, Slovenia, and Sincrotrone Trieste, Italy.*

^b *also at: Dipartimento di Fisica dell'Università di Trieste, Italy.*

F. Bisio, S. Terreni and M. Canepa

INFN and Dipartimento di Fisica dell'Università di Genova, Italy.

Islands of 1-2 nm lateral size and double layer height are formed when 1 monolayer (ML) of Fe is deposited on $\text{Cu}_3\text{Au}(001)$ at low temperature. We used the PhotoElectron Diffraction (PED) technique to investigate the atomic structure and chemical composition of these nanoislands just after the deposition at 140 K and after annealing at 400 K. We show that only bi-layer islands are formed at low temperature, without any surface segregation. After annealing, the Fe atoms are re-aggregated to form mainly tri-layer islands. Surface segregation is shown to be inhibited also after the annealing process. The implications for the film magnetic properties and the growth model are discussed.

PACS numbers: 61.14.Qp, 68.49.Jk, 68.55.Jk

arXiv:cond-mat/0109436v1 [cond-mat.mtrl-sci] 24 Sep 2001

*Corresponding Author: Luca Floreano, Surface Division, Laboratorio TASC-INFN, Basovizza, SS14 Km 163.5 I-34012 Trieste, Italy. Fax: +39-040-226767; E-mail: floreano@sci.area.trieste.it

The properties of nanometers size clusters of magnetic materials are subject of extended studies for their relevance in the miniaturization of memory storage devices. Both the reduced dimensionality and system size are responsible for magnetic behavior different from that observed in bulk materials. Self assembly on suitably chosen substrates is a well exploited root to control the structure and morphology, hence magnetization, of metal films. Much attention has been devoted to ultrathin Fe films, due to the possibility of stabilizing Fe in magnetic phases different from the bcc bulk ones, i.e. either superferromagnetic or antiferromagnetic, or even nonmagnetic.^{1,2} In particular, the $\text{Cu}_3\text{Au}(001)$ surface has been recently singled out as a good template to grow high spin Fe phases,^{3–5} due to the close matching between the Cu_3Au lattice constant (3.75 Å) and the equilibrium lattice constant for fcc ferromagnetic Fe (3.65 Å).

In fact, fcc Fe films on $\text{Cu}_3\text{Au}(001)$ are obtained with an increasing degree of tetragonal distortion as the thickness is increased, until a bcc-like phase is finally recovered.^{6–9} Previous research mostly dealt with the spin reorientation transition of the surface magnetization from out-of-plane to in-plane and its possible correlation with the structural transition from fcc to bcc.^{4,5} Here we will focus on the initial stages of growth, where Fe is expected to be pseudomorphic to the substrate, thus yielding the largest volume of its lattice cell, hence the highest magnetic moment.¹ While growth proceeds almost layer by layer at room temperature (RT),⁸ with a small amount of Au segregation,^{7,9} the formation of uniform size (on the nanometer scale length) flat bi-layer islands was recently observed by He atom scattering (HAS) after deposition of 1 ML of Fe at 140 K.¹⁰ Bi-layer nanoislands of this kind were also reported for a few metal on metal systems in the first monolayer range.^{11–13} Several mechanisms have been suggested to drive the bi-layer growth such as magnetostriction effects,¹² combination of strain and electron confinement,¹⁰ and a combination of strain and exchange processes.¹⁴ A better knowledge of the inner structure and chemical composition of these nanoislands would be helpful to understand the driving force for the bi-layer growth. Up to now these systems have been investigated by techniques such as HAS and scanning tunneling microscopy (STM) which only probe the outer surface valence charge density.

In the present work, we have exploited the experimental techniques available at the ALOISA beamline¹⁵ of the Elettra Synchrotron (Trieste, Italy) for a structural and chemical characterization of the islands formed after deposition of 1 ML of Fe at 140 K, and subsequent annealing to 400 K. Surface X-ray diffraction (XRD), X-ray specular reflectivity (XRR) and PED were previously used for a complete characterization of the Fe/ $\text{Cu}_3\text{Au}(001)$ system in a higher thickness range (3–36 Å).⁶ The same sample of Refs.^{6,7,10} has been used, further details about sample preparation are given elsewhere.^{6,16} After calibration, XRR allowed us to monitor the deposition of a single Fe ML with a high level of precision and repro-

ducibility. PED patterns have been taken to determine the structure of Fe islands and to check the occurrence of Au segregation at the Fe island surface. We measured the photoelectrons of the Fe $2p_{3/2}$ core-level at a Kinetic Energy of 231 eV. The PED polar scans have been measured by collecting the photoemission signal as a function of the emission angle θ , by rotating the electron analyzer in the scattering plane. The grazing angle was kept fixed at 4.5° , with the polarisation in transverse magnetic condition and the surface oriented with the $\langle 100 \rangle$ direction in the scattering plane.

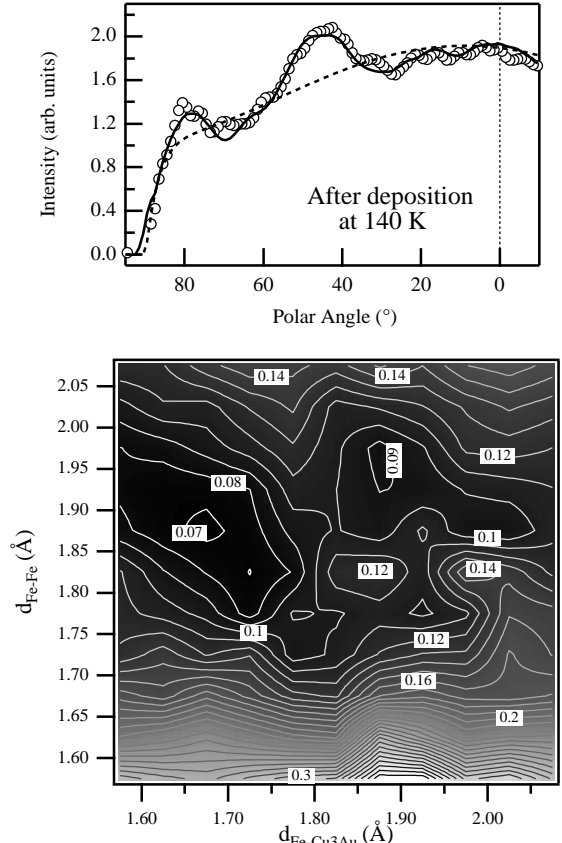


FIG. 1. Upper panel: PED polar scan taken along the $\langle 100 \rangle$ symmetry direction after the deposition at 140 K (open circles). The best-fit model (full line) of the bi-layer is reported, together with the best ISO background (dashed line). The surface normal is indicated by the vertical dotted line at 0° . Lower panel: R-factor analysis of the PED simulation for different values of the vertical spacing between the two Fe layers $d_{\text{Fe-Fe}}$ and the Fe-substrate layers $d_{\text{Fe-Cu}_3\text{Au}}$.

The photoelectron angular modulation is given by the superposition of two contributes: i) the diffractive atomic-position-dependent anisotropy term χ -function, which has been determined by multiple scattering calculations (MSCD code¹⁷ with hemispherical clusters of radius = 9.5 Å and about 170 atoms, Multiple-Scattering-order = 6, Rehr-Albers-Order = 2, Debye Temperature = 220 K and inner potential $V_0 = 10$ eV); ii) the

isotropic background $ISO(\theta)$ arising from the emission matrix element, sample attenuation, surface roughness, sample illumination and analyzer response, which have been described by an analytical expression.⁶ Both contributes have been compared to simulations by means of a reliability R-factor analysis.

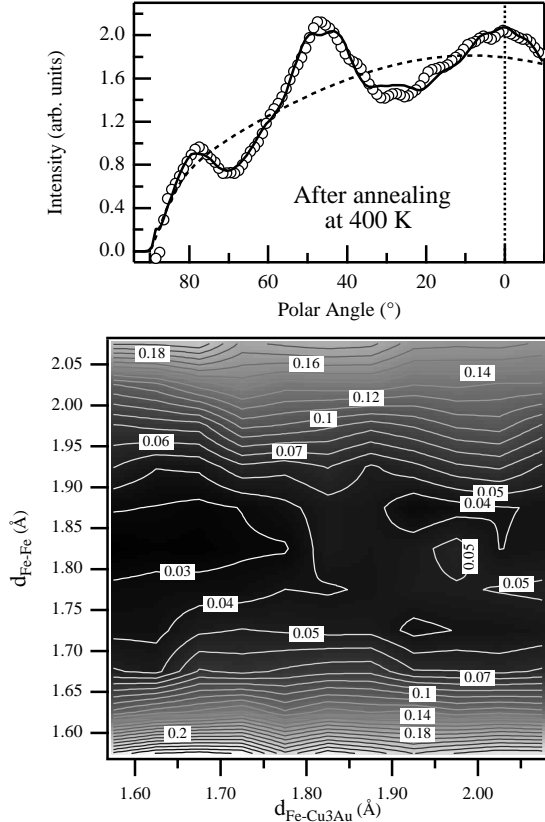


FIG. 2. Upper panel: PED polar scan taken along the $\langle 100 \rangle$ symmetry direction after annealing at 400 K and cooling to 140 K (open circles). The best-fit model (full line) of the tri-layer is reported, together with the best ISO background (dashed line). The surface normal is indicated by the vertical dotted line at 0° . Lower panel: R-factor analysis of the PED simulation for different values of the vertical spacing between the Fe layers d_{Fe-Fe} and the Fe-substrate layers d_{Fe-Cu_3Au} . Here the Fe interlayer spacing has been kept equal for both the first to second and the second to third Fe layer spacing.

A qualitative inspection of the polar scan taken after deposition at 140 K indicates the formation of a double layer fcc-like structure (see Fig. 1, upper panel). In fact, the anisotropy χ -function along the $\langle 100 \rangle$ direction is characterized by an intense peak at about 45° , which is the fingerprint of an fcc structure. At the same time, no diffraction features are observed along the surface normal; this can be ascribed to the fact that the third layer of the fcc structure is not formed yet. The polar scan, taken after annealing the film at 400 K for 5 minutes and cooling down to 140 K, is reported in the upper panel of Fig. 2. The experimental data display an over-

all increased anisotropy; in particular the increase of the anisotropy at the surface normal and at 45° is a clear hint of the formation of the third layer in the fcc structure.

The best-fits, shown in Figs. 1 and 2, have been obtained by keeping the lateral lattice parameter fixed to the substrate value of 2.65 \AA (i.e. the half-diagonal of the $Cu_3Au(100)$ lattice constant), according to the XRD indication from ref.⁶. The separation between the Fe-Fe and Fe-substrate layers (d_{Fe-Fe} and d_{Fe-Cu_3Au} , respectively) have been used as fitting parameters. In the case of bi-layer islands, we found a certain degree of correlation between d_{Fe-Fe} and d_{Fe-Cu_3Au} , thus yielding a good estimate of the total island height $d_{Fe-Fe} + d_{Fe-Cu_3Au} \sim 3.55 \text{ \AA}$, but a rather large uncertainty in the individual parameters $d_{Fe-Fe} = 1.87 \pm 0.1 \text{ \AA}$ and $d_{Fe-Cu_3Au} = 1.67 \pm 0.1 \text{ \AA}$. In the case of tri-layer islands, the spacing between Fe layers was found to be $d_{Fe-Fe} = 1.83 \pm 0.05 \text{ \AA}$ for both the topmost and inner Fe layers (i.e. no surface relaxation was detected). The latter value corresponds to the vertical lattice spacing of the fcc substrate, in full agreement with the value previously obtained for an Fe film of 3 \AA nominal thickness (about 2 ML).⁶ The Fe-substrate separation is not equally well determined, even if it points to a contracted value $d_{Fe-Cu_3Au} = 1.65 \pm 0.15 \text{ \AA}$ for the tri-layer islands too.

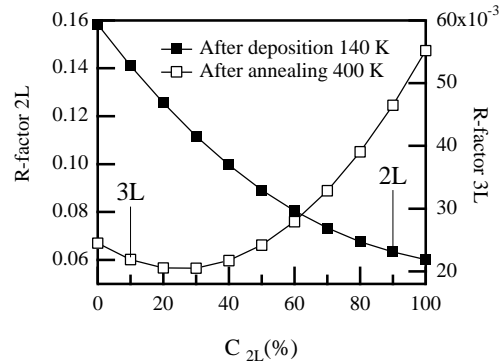


FIG. 3. R-factor analysis for evaluating the concentration of bi- and tri-layer Fe islands. The comparison is made with a linear combination of double and triple layer Fe models for the low temperature deposition (filled squares) and after annealing at 400 K (open squares). The concentration C_{2L} is the weight in % of the double layer model.

Once obtained the film structure, the height distribution of the islands for each film has been determined by fitting the polar scans to a linear combination of the χ -functions calculated for the double and triple layer films:

$$\chi = C \cdot \chi_{2ML} + (1 - C) \cdot \chi_{3ML}, \quad (1)$$

where $C = C_{2L}$ plays the role of "concentration" of the double layer film. From the R-factor analysis in Fig. 3, we can say that no tri-layer islands are formed after the deposition at LT (as expected by the inspection of the

polar scan in the upper panel of Fig. 1). The comparison to the experimental data taken after the annealing process (open squares) presents a minimum of the R-factor at about $C_{2L} = 25\%$. Therefore, after the annealing process there is a majority amount ($\sim 75\%$) of tri-layer islands. The results for both as-deposited and annealed films are in full agreement with previous HAS analysis.¹⁰ The eventual presence of single layer height Fe islands cannot be taken into account by this kind of PED analysis, but this hypothesis can be excluded on the basis of the analysis of the HAS data.

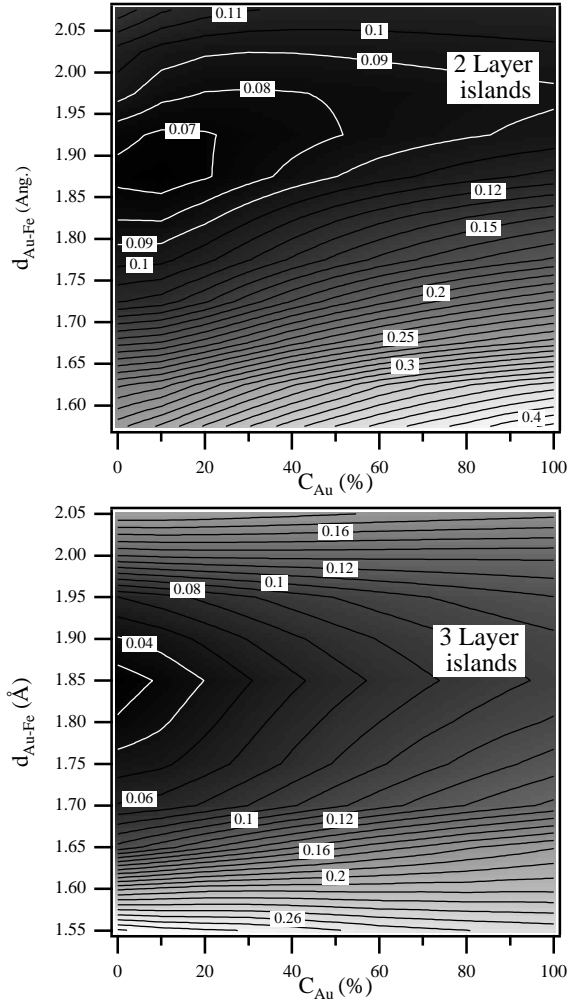


FIG. 4. R-factor analysis for different extent of Au segregation. In the upper (lower) panel the experimental data of the film just after deposition (after annealing) is compared with a linear combination of Au-substituted model and an all-Fe model (see text). The concentration C_{Au} is the weight in % of the Au-substituted model.

Next we checked for the chemical composition of the Fe islands. The presence of Au atoms on top of the Fe film can be revealed since they would yield an overall increase of the Fe PED pattern anisotropy, due to the

Au atom cross section which is larger than the Fe atom one. In the simulated best-fit models we substituted the Fe atoms of the topmost layer with a full layer of Au atoms and calculated the corresponding χ -functions. The resulting χ -functions of each Au-substituted film were then combined with the χ -functions of the corresponding all-Fe-model, using eq. 1, where $C = C_{Au}$ now is the concentration of the Au-substituted film. The R-factor as a function of C_{Au} and of the height d_{Au-Fe} of the Au layer on top of the Fe one is reported in Fig. 4. As can be seen, no Au segregation can be inferred by the PED analysis not even after the annealing, therefore the main effect of the annealing process is to favor the atoms on the surface to form thicker islands with the same fcc structure.

Our R-factor analysis cannot be extended to check for Cu segregation, since the Cu scattering cross-section is close to the Fe one. On the other hand, Cu segregation is known to be negligible for the Fe/Cu(100) system at LT,^{11,18} while a full Au layer was observed to segregate on top of Fe films grown on Au(100) for many Fe layers.¹⁹ Therefore the segregation of Cu atoms seems unlikely when the segregation of Au is inhibited.

Beyond the chemical composition of Fe nanoislands, we remark the different film morphology that can be achieved as a function of the substrate temperature during and after the growth. The LT deposition of 1 ML of Fe yields a distribution of homogeneously sized bi-layer nanoislands, whereas multilayer growth has been reported at RT for a similar coverage, with the first layer close to percolation limit and several third layer islands.⁸ The magnetic measurements reported in the literature are also different between films grown at RT^{4,6,8} and films grown at LT, with or without annealing.^{5,9} A magnetization oriented perpendicularly to the surface is reported for Fe films, obtained by RT annealing 1 ML of Fe deposited at LT.^{4,5} A larger Fe amount is always required for the magnetization onset, when the film is grown at RT.^{4,5} A very similar magnetic behavior is reported for thin Fe films grown on Cu(001).²⁰ In the latter case, the onset of the magnetization (normal to the surface) occurs at a critical Fe coverage, which decreases as the substrate deposition temperature is decreased. A minimum critical coverage of 1 layer equivalent was eventually reached upon deposition at 190 K,²⁰ where only bi-layer islands are observed,¹² like in the Fe/Cu₃Au system. We can conclude that the onset of the perpendicular magnetization cannot be simply related to the formation of an extended and connected single Fe layer on the substrate (as observed for Fe on W(110)²¹), but rather to the formation of an Fe bulky volume. Due to the scattering of data reported in the literature, it is not possible to rigorously state the onset of magnetization before the coalescence of LT bi-layer islands sets in. However, we remark that, even if the magnetization onset is delayed up to the bi-layer percolation limit, the substrate Fermi electrons must play a fundamental role in driving the coherent orientation of the Fe island spin (similarly to the magnetic

exchange coupling of layered systems²²), because of the intrinsic inhomogeneity of the coalescence process.

The LT morphology cannot be described by a kinetic model based on the interplay between intra- and inter-layer diffusion coefficients. The Schwoebel barrier for the interlayer diffusion is hardly overcome at RT.²³ At LT the Fe atoms landing on top of the first layer are efficiently trapped in the second layer, but those landing on top of the second layer never form a third one, rather they are incorporated in the second layer leading to a flat bi-layer island morphology. A self-induced magnetostriction effect⁸ can be excluded on the basis of energetics arguments. If the kinetic barrier for the atom incorporation is of the order of the Schwoebel barrier (i.e. of the order of eV²³), the nanoisland strength of magnetostriction should be of many meV/atom, which is almost two orders of magnitude larger than typical magnetostriction forces.²⁴

Very recently, the formation of bi-layer Co islands on Cu(111) was explained by a theoretical model predicting the collapse of single layer islands above a critical size due to the interplay between the excess of strain and exchange processes.¹⁴ In fact, the excess of Fe surface energy is lower when considering the (100) surface of both Cu and Cu₃Au.²⁵ Moreover, segregation, which would relieve the surface strain to stabilize the island growth, is shown to be absent, when the bi-layer nanoislands are formed at LT.

The additional energy excess required to stabilize the Fe nanoislands on Cu₃Au might arise from the quantum confinement of the Fe *d*-electrons, like in the model of LT electronic growth proposed by Zhang and coworkers.²⁶ In this mean field model, islands of “magical” thickness are formed due to the balance between the stress at the interface, the charge transfer and the quantum size effects (QSE). While typical of metals grown at LT on semiconductors, structural QSE have been also reported for Pb on Cu(111).²⁷ Finally, the manifestation of electronic phenomena in the low temperature phases of Fe on Cu₃Au seems consistent with the thickness induced oscillations (~ 3.7 Å period) of the magnetization observed on the Fe/Cu(100) system at LT.²⁰ These oscillations were in fact related to the quantum well states in the Fe film,²² i.e. to the manifestation of QSE.

L. F. is grateful to G. Rossi and C. Carbone for useful discussions. Funding from INFN and from the Italian Ministero dell’Università e Ricerca Scientifica (Cofin99 Prot. 990211848 and 9902112831) are gratefully acknowledged.

¹ E.G. Moroni, G. Kresse, J. Hafner, and J. Furthmüller, Phys. Rev. B **56**, 15629 (1997).

² V.L. Moruzzi, P.M. Marcus, and J. Kübler, Phys. Rev. B

- 39**, 6957 (1989); P.M. Marcus, V.L. Moruzzi, and S.L. Qiu, Phys. Rev. B **60**, 369 (1999).
- ³ R. Rochow *et al.*, Phys. Rev. B **41**, 3426 (1990).
- ⁴ M.-T. Lin *et al.*, Phys. Rev. B. **55**, 5886 (1997).
- ⁵ B. Feldmann, B. Schirmer, A. Sokoll, and M. Wuttig, Phys. Rev. B. **57**, 1014 (1998).
- ⁶ F. Bruno, S. Terreni, L. Floreano, D. Cvetko, P. Luches, L. Mattera, A. Morgante, R. Moroni, A. Verdini, and M. Canepa, to be published (<http://arXiv.org/abs/cond-mat/0103458>); F. Bruno *et al.*, Appl. Surf. Sci. **162-163**, 340 (2000).
- ⁷ P. Luches, A. Di Bona, S. Valeri, and M. Canepa, Surf. Sci. **471**, 32 (2000).
- ⁸ M.-T. Lin *et al.*, Surf. Sci. **410**, 290 (1998).
- ⁹ B. Schirmer, B. Feldmann, and M. Wuttig, Phys. Rev. B. **58**, 4984 (1998).
- ¹⁰ M. Canepa, P. Cantini, C. Mannori, S. Terreni, and L. Mattera, Phys. Rev. B **62**, 13121 (2000).
- ¹¹ K.E. Johnson, D.D. Chambliss, R.J. Wilson, and S. Chiang, Surf. Sci. **313**, L811 (1994).
- ¹² J. Giergiel, J. Shen, J. Woltersdorf, A. Kirilyuk, and J. Kirschner, Phys. Rev. B **52**, 8528 (1995).
- ¹³ J. de la Figuera, J.E. Prieto, C. Ocal, and R. Miranda, Phys. Rev. B **47**, 13043 (1993).
- ¹⁴ L. Gómez *et al.*, Phys. Rev. Lett. **84**, 4397 (2000).
- ¹⁵ L. Floreano *et al.*, Rev. of Sci. Inst. **70**, 3855 (1999); R. Götter *et al.*, Nucl. Instrum. Methods A **467-468**, 1468 (2001); an updated presentation of the beamline can be found at <http://tasc.area.trieste.it/tasc/lds/aloisa/aloisa.html>.
- ¹⁶ C. Mannori *et al.*, Surf. Sci, **433**, 307 (1999); C. Mannori *et al.*, Europhysics Lett. **45**, 686 (1999).
- ¹⁷ MSCD is freely distributed by Y. Chen and M.A. Van Hove at: “<http://electron.lbl.gov/mscdpack/mscdpack.html>”; also see Y. Chen *et al.*, Phys. Rev. B **58**, 13121 (1998).
- ¹⁸ M.T. Kief and W.F. Egelhoff, Phys. Rev. B **47**, 10785 (1993).
- ¹⁹ S.A. Kellar *et al.*, Phys. Rev. B **57** 1890 (1998); R. Opitz, S. Löbus, A. Thissen, and R. Courths, Surf. Sci. **370**, 293 (1997).
- ²⁰ Dongqi Li, M. Freitag, J. Pearson, Z.Q. Qiu, and S.D. Bader, Phys. Rev. Lett. **72**, 3112 (1994).
- ²¹ H.J. Elmers *et al.*, Phys. Rev. Lett. **73**, 898 (1994).
- ²² J.E. Ortega, F.J. Himpsel, G.J. Mankey, and R.F. Willis, Phys. Rev. B **47**, 1540 (1993); M.D. Stiles, Phys. Rev. B **48**, 7238 (1993).
- ²³ J.A. Stroschio, D.T. Pierce, and R.A. Dragoset, Phys. Rev. Lett. **70**, 3615 (1993).
- ²⁴ P. Bruno, *Physical origins and theoretical models of magnetic anisotropy*, in the proceedings of the 24th IFF-Ferienkurs/1993 on *Magnetismus von Festkörpern und Grenzflächen*, p. 24.1, Forschungszentrum Jülich GmbH (1993).
- ²⁵ L. Vitos, A.V. Ruban, H.L. Skriver, and J. Kollar, Surf. Sci. **411**, 186 (1998); Ch.E. Leka, N.I. Papanicolaou, and G.A. Evangelakis, Surf. Sci. **479**, 287 (2001).
- ²⁶ Z. Zhang, Q. Niu, and C.-K. Shih, Phys. Rev. Lett. **80**, 5381 (1998); K.-J. Jin, G.D. Mahan, H. Metiu, and Z. Zhang, Phys. Rev. Lett. **80**, 1026 (1998).
- ²⁷ J. Braun and J.P. Toennies, Surf. Sci. Lett. **384**, L858 (1997).